Microporous and Mesoporous Materials 343 (2022) 112156

Contents lists available at ScienceDirect

Microporous and Mesoporous Materials

journal homepage: www.elsevier.com/locate/micromeso

Application of a tailorable carbon molecular sieve to evaluate concepts for the molecular dimensions of gases

Ansgar Kretzschmar [a,b,*], Victor Selmert [a,b], Hans Kungl [a], Hermann Tempel [a], Rüdiger-A. Eichel [a,b]

[a] Forschungszentrum Jülich GmbH, Institute of Energy and Climate Research – Fundamental Electrochemistry (IEK-9), 52425, Jülich, Germany
[b] RWTH Aachen University, Institute of Physical Chemistry, 52056, Aachen, Germany

ARTICLE INFO

Keywords:
Molecular sieve
Kinetic diameter
Critical diameter
Carbon
Gas separation

ABSTRACT

Molecular sieves have attracted considerable interest for gas separation applications due to their ability to discriminate substances by their molecule's size. To predict if a molecular sieve is suitable for a specific separation problem an accurate measure of the molecular sizes is called for. Furthermore, a high precision in estimations for molecular dimensions is needed for the characterization of materials using molecular probes. In this work, different popular concepts to estimate the size of a gas molecule, specifically Breck's kinetic diameter, the critical diameter and molecular dimensions by Webster (MIN-1) are discussed. These concepts are evaluated using a tailorable carbon molecular sieve. It is concluded, that the widely used kinetic diameter has some drawbacks to determine the accessibility of pores. Finally, recommendations for alternatives from existing literature are presented.

1. Introduction

1.1. Motivation

Molecular sieves are materials that can discriminate between substances by their size on molecular level. To achieve such a sieving effect, these materials exhibit an extremely narrow pore system in the size range of individual molecules, i.e, sub-nanometer dimensions. There is a number of materials available that fulfill these requirements. Among those porous materials employed as molecular sieves, zeolites play a most important role. Nonetheless, metal-organic frameworks (MOFs), polymers and carbons are frequently reported as well. Zeolites and MOFs exhibit a high stability and very uniform pore size distribution but bind polar substances very strong. In contrast, carbon molecular sieves usually have a less defined structure but their regeneration is less energy consuming. With appropriate synthesis methods, molecular sieves can be tailored for many specific separation applications.

There are many applications for molecular sieves, ranging from the drying of solvents to the purification of different isomers of hydrocarbons or the separation of oxygen from air. For example, the potassium-substituted form of zeolite A is a very effective drying agent for protic organic solvents like methanol [1,2], whereas the sodium-base zeolite A is employed to dry aprotic solvents [3]. In these drying applications, the comparatively small water molecule is selectively adsorbed in narrow pores of the molecular sieves, whereas the larger solvent molecules are excluded from entering the pore system by their size. Furthermore, these zeolites may be employed for humidity control in air conditioning systems [4]. Beside removing water from air, a carefully adjusted carbon molecular sieve can separate nitrogen and oxygen [5–8], which is the preferred method to generate technical nitrogen and oxygen from air in a small to medium scale [7,9]. The capture of CO_2 from its mixture with methane (relevant for biogas or natural gas) has been reported as well for zeolite [10–12] and carbon molecular sieves [13]. In petrochemistry, zeolites are well known for their application in catalysis, most importantly in the Fluid Catalytic Cracking (FCC) process [14]. Nevertheless, zeolites can also be employed to separate different isomers of hydrocarbons [15] or paraffins and olefins [14].

From a process perspective, molecular sieves can be employed in an adsorption process that requires alternating adsorption and regeneration steps (pressure or temperature swing adsorption) or, when continuous pores are present, serve as (component of) a membrane. Both processes correspond to different separation mechanisms in molecular

* Corresponding author. Forschungszentrum Jülich GmbH, Institute of Energy and Climate Research – Fundamental Electrochemistry (IEK-9), 52425, Jülich, Germany.
E-mail address: a.kretzschmar@fz-juelich.de (A. Kretzschmar).

https://doi.org/10.1016/j.micromeso.2022.112156
Received 14 April 2022; Received in revised form 29 July 2022; Accepted 1 August 2022
Available online 4 August 2022

sieves, which can be either a real size exclusion effect or a kinetic separation, where the smaller molecule diffuses much faster through a pore of a given size. In a practical application, there will usually be a trade-off between the high selectivity of a pure molecular sieve effect and sufficient adsorption or diffusion rates in larger pores. More detailed discussions of these and other separation mechanisms can be found in the review literature, especially on gas separation membranes [16–18]. This work focuses on the size exclusion effect in equilibrium rather than on kinetic effects.

Aside from the separation of various molecules from each other with the help of a molecular sieve, the sieving effect can also be used to characterize the molecular sieve itself with a number of adsorbate molecules of a given size. Before modern computational chemistry methods for the calculation of pore size distributions from gas adsorption isotherms became available, the molecular sieve effect was used to evaluate the pore size distribution of a given material with different adsorptives, giving information on the pore volume in a specific size range between two adsorptives of different dimensions ("molecular probe method") [19–23]. Molecular packing effects of different adsorptives can also be studied to verify calculated pore size distributions [24].

The precision of these methods greatly depends on the values used for the molecular size of gas molecules. To evaluate and compare different concepts for molecular dimensions is the aim of this work. First of all, common concepts for a molecular diameter calculation from the literature are presented. Secondly, a tailorable molecular sieve from previous work is introduced and the methodology is explained, how an adjustable molecular sieve enables to evaluate different approaches to estimate molecular sizes. Subsequently, the suitability of different concepts for molecular sizes are evaluated for typical application scenarios of molecular sieve adsorbents, using experimental results obtained with the tailorable molecular sieves. Lastly, remaining inconsistencies observed for some concepts are discussed individually, again making use of experimental results from the tailorable molecular sieve.

1.2. Concepts for the molecular dimension

For all applications listed above, accurate measures for the size of molecules are required to give a quick estimate if a certain mixture of gases can be separated with a specific molecular sieve. There are several methods available that intend to give an average value of the size of a molecule to assess the accessibility of a molecule into a pore. It must be acknowledged, however, that any fixed value describing the dimension on molecular level must be considered with caution due to the continuous decrease of electron density around a molecule with increasing distance from its center and a potential polarizability [20,21]. In the following, three representative sets of values for molecular dimensions from the literature with different approaches will be presented. Fig. 1 provides a schematic overview on these three common approaches.

First of all, collision diameters can be deducted from macroscopic experimental data like the second virial coefficient [25] via gas density measurements or gas viscosity [26] (Fig. 1a). One of the most frequently cited set of values are the *kinetic diameters* collected by Breck [27] in his book from 1974. These kinetic diameters are based on experimental data for the second virial coefficient. Many of the values in Breck's collection are taken from the older book of Hirschfelder, Curtiss and Bird [25] from 1964, where the procedure to obtain diameters from virial coefficient data is explained in detail. In short, the virial coefficient B can be expressed as a collection of spheres surrounded by an adsorption potential. With a suitable adsorption potential function and an experimental value for B, characteristic parameters of the potential function can be calculated. For nonpolar and spherical molecules, the Lennard-Jones potential is commonly applied. For polar molecules, the Stockmayer potential [28] may be employed. The most important equations are also listed in the supporting information. To account for some irregularities, Breck made manual adjustments to his list. For example, Breck [27] noted that the diameter of CO_2 obtained from the Lennard-Jones potential (405 p.m.) is too large to explain experimental results with zeolite A and recommends to use an older value derived from data collected by Pauling [29].

Considering the macroscopic approach for the calculation of the molecular dimension, only a single average value can be obtained with this method [21,27,30]. Some drawbacks of this method to describe a molecular sieve effect are obvious. For asymmetric molecules, a single parameter describing an average value for three dimensions may be insufficient to describe their ability to access a certain pore system [21,

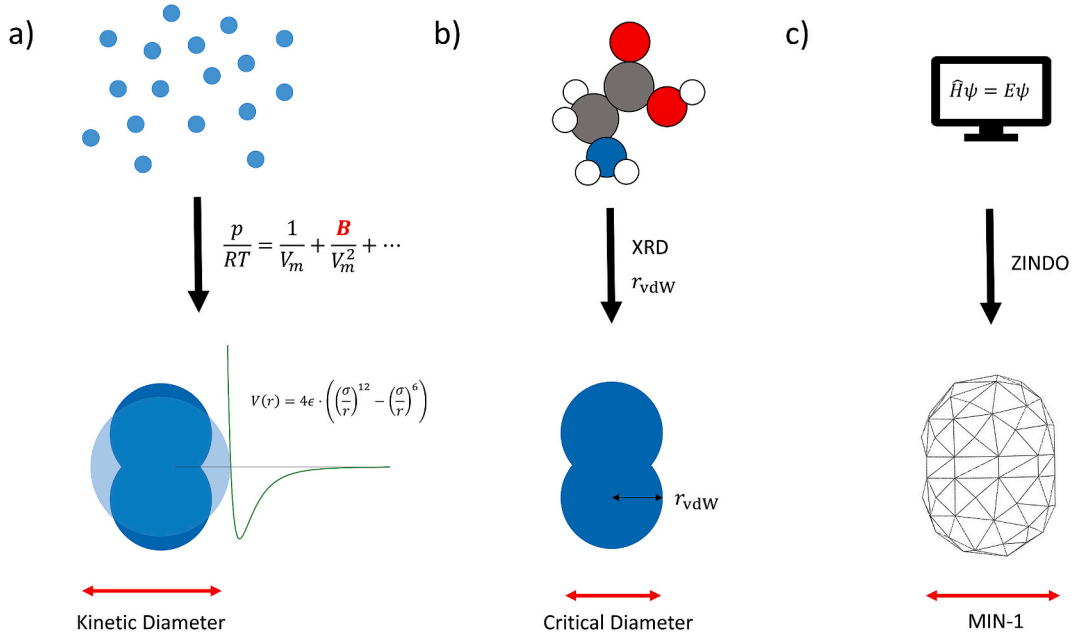

Fig. 1. Schematic overview of different methods to determine molecular dimensions for an exemplary diatomic gas molecule. First, the approach via macroscopic experimental data like virial coefficients or gas viscosity (a). Secondly, geometric considerations with van der Waals-radii (r_{vdW}) derived from diffraction data (b) and thirdly, computational chemistry approaches (c).

30]. Given that Breck collected most of his kinetic diameters from older work, it must be emphasized that much of the underlying experimental data dates back to the 1930s or even earlier. Some of these drawbacks of Breck's kinetic diameters are discussed in literature, for example for pore size analysis [20,21] (equilibrium data) or for the selectivity prediction in membranes [16] (kinetics, diffusion). In both cases, criticism is based mostly on the fact that the kinetic diameter does not appropriately consider shape anisotropy. Furthermore, concern arises from inconsistencies of kinetic diameters obtained from virial coefficient data and viscosity data [16].

In this context, it must be noted that the term "kinetic diameter" is not restricted to the values collected by Breck. There are more collections of "kinetic diameters" or "effective kinetic diameters" with different experimental procedures that are, however, less commonly used in this context [31,32]. As another example for macroscopic approaches, molecular dimensions derived from gas viscosity data are often called Lennard-Jones diameters [16,26,33], although the Lennard-Jones potential is also used to determine kinetic diameters from virial coefficients. Frequently cited Lennard-Jones diameters by Svehla [26] are listed in the Supporting Information.

Another approach to determine molecular dimensions is to construct a molecule from bond angles and van der Waals-radii (Fig. 1b). A frequently mentioned set of values are the so-called *critical diameters*. These values were listed by Grubner, Jiru and Ralek in 1968 in their book on molecular sieves [34,35] and appear in several textbooks on chemical engineering [36–39] as well as online resources [40,41]. For spherical adsorptives such as noble gases or methane, the critical diameter is simply defined as the diameter of the sphere surrounding the molecule [34]. For diatomic molecules (H_2, N_2, O_2, …), the critical diameter is the diameter of the smallest circle that is perpendicular to the length axis of the molecule [34]. The critical diameter of tetrahedral (CCl_4) and octahedral (SF_6) molecules is defined as the diameter of the smallest circle around the triangle of the tetrahedron and the square base of the octahedron, respectively. According to Grubner et al. asymmetric molecules can be described by the diameter of the smallest sphere surrounding the molecule [34]. Primary sources for the employed van der Waals-radii and bond angles are, however, not given, neither by Grubner et al. nor by the other works listing critical diameters.

Some of these values for simple molecules, however, appear to be based on the early works of Barrer on zeolites [42], who calculated *critical dimensions* for H_2, O_2, N_2 using the van der Waals-radii listed in a book by Pauling [29]. These van der Waals-radii are derived from averaged diffraction data of organic molecules and used to make a simple geometric construction of the molecule (Fig. 1b). The critical diameter is then the shortest distance from edge to edge of the molecule. To give a size estimate for noble gases such as Ar, crystallographic data was used by Barrer [43,44]. In contrast to kinetic or Lennard-Jones diameters, problems arising from the evaluation of highly asymmetric molecules due to the insufficient description of the molecule's size with a single parameter can be mitigated. To avoid confusion, it must be emphasized that the term *critical diameter* is sometimes used for other lists of molecular dimensions [45], even though the list by Grubner et al. [34] is far more popular, given its presence in several textbooks [36,38,39] and Ullmann's encyclopedia of industrial chemistry [37].

To further address the issue of insufficient descriptions of molecules with different lengths in different dimensions, Webster et al. [30,46–48] proposed additional values based on calculations of the electronic structure with the program ZINDO [49] (Fig. 1c). Using the subroutine GEPOL [50–52], a van der Waals molecular surface was calculated as envelope around the adsorptive, which is basically a set of intersecting spheres centered in the nuclei of the individual atoms [48]. Finally, molecular sizes in different dimensions were calculated by connecting the outermost points of the molecular surface. MIN-1 is the smallest diameter of the molecule in any direction, while MIN-2 represents the molecule's smallest diameter perpendicular to MIN-1.

Webster lists molecular sizes for three different dimensions, which allows to evaluate size exclusion effects in a more sophisticated way. For slit pores as found in carbon molecular sieves as the one studied here, only the smallest length of a molecule is relevant because the depth and length of the pore are considerably larger than its width. Consequently, only the value MIN-1 by Webster will be considered in this work. MIN-2 may be used for adsorbents with cylindrical pores, where both length and width play a role for the accessibility of the pore [30]. Consideration of the third dimension (MIN-3) may be of interest for the analysis of diffusion [30].

Table 1 gives an overview on frequently used sets of values for the size of chosen molecules.

There are only few publications available that present sufficient data to allow for a general comparison of these different approaches. Usually, these works present adsorption results of various gases on a single material, be it for the characterization of adsorbents [61] or kinetic effects in separation membranes [62,63]. For example, Madani et al. studied the behavior of several adsorptives with different kinetic diameters on a microporous carbon [64,65] and evaluated the adsorption mechanisms as well as the consistency of Gurvich volumes. However, due to the absence of a molecular sieve effect, some inconsistencies [64] observed in the obtained Gurvich volumes cannot be explained by the choice of the molecular diameter concept. Liu et al. presented a high throughput approach to characterize 15 carbonaceous molecular sieves with 9 adsorptives with different kinetic diameters [61]. Equilibrium capacities and kinetic data was presented in a way to account for some industrially relevant separation problems. A discussion of the validity of the molecular diameter was not aimed at. Traa and Weitkamp discussed molecular sieving in zeolites with a focus on hydrocarbons in great detail [21,22]. They recommend the concept of Webster et al. [30,46–48] over the kinetic diameter due to its ability to account for different dimensions. In addition, Yampolskii discussed some concepts for the molecular diameter in his books, focusing on diffusion in gas separation membranes [16,66]. However, as the separation mechanism is not necessarily limited to molecular sieving, kinetic effects in gas separation membranes can be complex to assess.

To directly compare different concepts for the molecular diameter without having to consider kinetic effects, a material is helpful which can be tailored to different pore sizes in the desired regime of ultramicropores, which is addressed in this work.

2. Materials and methods

2.1. Electrospun PAN-based carbon nanofibers as a tailorable molecular sieve

In a previous work, electrospun PAN-based carbon fibers were presented [67] that were carbonized in a range from 600 to 1100 °C and were not activated by any additional reactant. The surface chemistry was evaluated with elemental analysis and XPS, whereas the pore structure was evaluated with Ar and CO_2 adsorption experiments [67]. In the Ar adsorption experiments, Type I isotherms with extremely slow adsorption kinetics were obtained for carbonization temperatures of 600 and 700 °C, indicating an ultramicroporous material. At higher carbonization temperatures, the isotherm shape changed to Type II, i.e., a nonporous surface. Similar results were obtained in CO_2 adsorption experiments. However, the change in isotherm shape was shifted to a higher carbonization temperature [67]. These results were explained with a carbon molecular sieve model:

Depending on the carbonization temperature, gas molecules with different dimensions can enter or are excluded from the ultramicropores in the fiber structure. More specifically, both Ar (at 87 K) and CO_2 (at 273 K) can access the pores of fibers carbonized at 600 °C. When elevating the carbonization temperature to 800 °C, CO_2 can still enter the pores while Ar is excluded by its size. For an even higher carbonization temperature of 1000 °C both gases cannot access the

Table 1
Overview on molecular dimensions for selected adsorptives. Kinetic diameter, critical diameter and MIN-1. If available, primary sources are listed as reference. Some additional, less commonly used lists of values for the molecular size [16,26,31,33,53–58] obtained with various methods can be found in the Supporting Information. The adsorptives printed in bold letters were used in this work.

Molecule	Critical Temperature [K]	Kinetic Diameter [pm] (Breck [27])	Ref.	MIN-1 [pm] (Webster [30, 46–48])	Ref.	Critical Diameter [pm] (Grubner [34,35])	Ref.
He	5	260	[55]	–	–	200	[34]
Ne	44	275	[25]	–	–	320	[34]
Ar	**151**	**340**	[25]	**351**	[47]	**383**	[34]
Kr	209	360	[25]	–	–	394	[34]
Xe	290	396	[25]	404	[47]	437	[34]
N_2	**126**	**364**	[59]	**299**	[30]	**300**	[34] ([42])
O_2	**155**	**346**	[25]	**293**	[30]	**280**	[34] ([42])
H_2	**33**	**289**	[25]	**-**	**-**	**240**	[34] ([42])
CO	**133**	**376**	[25]	**328**	[30]	**320**	[34]
CO_2	**304**	**330**	[27]	**319**	[30]	**280**	[34]
N_2O	**310**	**330**	[27]	**303**	[5]	**-**	**-**
H_2O	**647**	**265**	[25]	**292**	[30]	**260**	[34]
NH_3	**405**	**260**	[25]	**311**	[30]	**380**	[34]
SO_2	431	360	[27]	337	[30]	–	–
SF_6	319	550	[25]	487	[30]	606	[34]
CH_4	**191**	**380**	[25]	**383**	[30]	**400**	[34]
C_2H_2	308	330	[27]	332	[5]	240	[34]
C_2H_4	**282**	**390**	[27]	**328**	[5]	**425**	[34]
C_2H_6	**305**	**410**[a]	[60]	**381**	[30]	**444**	[34]
C_3H_6	225	450	[27]	–	–	–	–
C_3H_8	**370**	**430**	[27]	**402**	[47]	**489**	[34]
C_6H_6	562	585	[27]	328	[30]	560	[34]
cyclo-C_6H_{12}	554	600	[27]	498	[30]	–	–

[a] Not listed in the original collection by Breck.

ultramicropores and the fibers behave like a simple nonporous surface [67]. This effect was explained by narrowing pores with increasing carbonization temperature and was confirmed by a kinetic analysis of CO_2 adsorption [68]. The structural changes during carbonization of the material have been examined as well in TEM studies [69,70]. In a recent publication, the separation performance of the electrospun PAN-based carbon nanofibers was evaluated in a dynamic flow system [71]. The breakthrough behavior was evaluated, along with the long-term stability over 300 cycles of adsorption and desorption [71].

It is expected that the observed size exclusion effect found for Ar and CO_2 can be applied to any other gas with molecules in the same size range. For each gas, there must be a specific *carbonization temperature threshold*, at which the adsorption capacity changes from high (the gas molecule can enter the pores) to low (the gas molecule is excluded from adsorption by its size). By measuring a set of adsorption isotherms for different carbonization temperatures for a specific gas, it shall be possible to determine the carbonization temperature threshold. If this is performed for a sufficient number of different gases, these thresholds can then be correlated to the molecular sizes listed above. The resulting value pairs then enable to draw two important conclusions:

1. The different concepts for determining the molecular size listed above can be qualitatively evaluated on a single carbon material.
2. When a concept for evaluating molecular sizes is found that satisfactorily describes the behavior of different gases on the electrospun PAN-based carbon fibers, it can be used to predict if they are suitable for a specific separation problem.

3. Experimental

PAN-based electrospun carbon nanofibers were prepared as described elsewhere [67,68]. Briefly, 8 g of Polyacrylonitrile ($M_W = 150'000$, BOC Science, USA) were dissolved in 72 g DMF (VWR Chemicals, Germany). The resulting solution was electrospun in an electrospinning device (IME Technologies, The Netherlands) at constant climate conditions (25 °C, 30% relative humidity). The obtained PAN nanofiber mats were stabilized in air for 15 h at 250 °C and carbonized in Argon atmosphere for 3 h at various temperatures from 600 to 1100 °C.

Isotherms and equilibration curves were obtained on an Autosorb iQ2 device equipped with three pressure transducers for each station (1 ktorr, 10 torr, 0.1 torr) and a Cryocooler (Quantachrome, USA). The obtained CNF mats were cut into small pieces and transferred into a glass tube. The samples were degassed under vacuum for 8 h at 200 °C. The sample weight was determined by calculating the difference of the weight of the filled and empty sample tube. All gas adsorption measurements were performed on the same sample series.

Gas adsorption isotherms were recorded in VectorDose™ mode. The gas purities are listed in Table S2.

4. Results

4.1. Carbonization temperature threshold

To evaluate the concepts for molecular size, isotherms of 13 gases on carbon fibers carbonized at 6 different temperatures in steps of 100 °C between 600 and 1100 °C were recorded at a temperature of 273 K. These isotherms are shown in the Supporting Information. For each gas, a carbonization temperature threshold was defined as the average of the highest carbonization temperature with high capacity and the lowest carbonization temperature with low capacity. In many isotherm sets, especially for subcritical gases (see Table 1), there may be an intermediate isotherm with extremely slow adsorption kinetics, which is then taken as the carbonization temperature threshold. As examples, the Ar and CH_4 sorption isotherms are shown in Fig. 2.

For the Ar adsorption at 273 K, the highest carbonization temperature with a high adsorption capacity of 0.4 mmol/g is 800 °C. The lowest carbonization temperature with a low capacity (about 0.02 mmol/g) is 900 °C. Hence, the average value of 850 °C is chosen as carbonization temperature threshold for Ar. For CH_4 adsorption at 273 K, the highest carbonization temperature without a reduction in adsorption capacity is

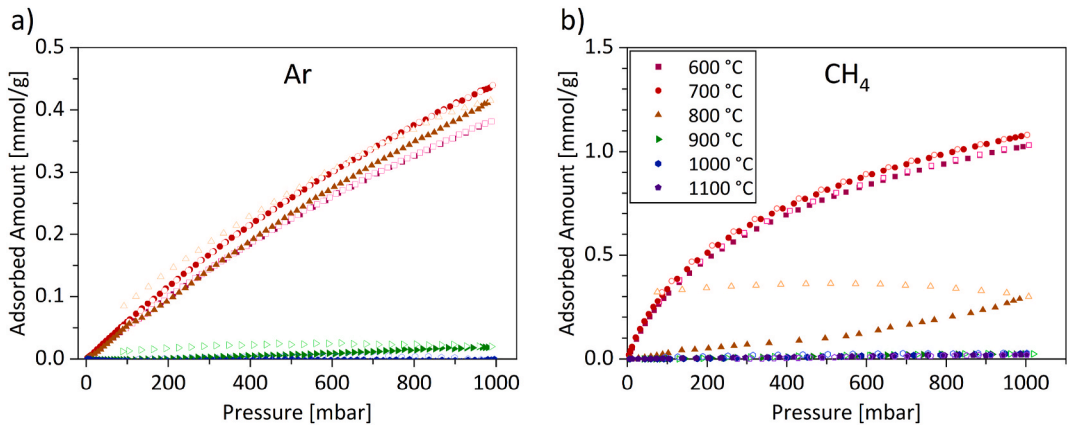

Fig. 2. Ar (a) and CH_4 (b) adsorption isotherms of electrospun carbon nanofibers prepared at different carbonization temperatures in a range from 600 to 1100 °C, measured at 273 K. Adsorption is shown as filled symbols, desorption as empty symbols. The color-coding is resolved in the legend in b. (For interpretation of the references to color in this figure legend, the reader is referred to the Web version of this article.)

700 °C. For 900–1100 °C, the adsorption capacity is much lower. The isotherm of the sample carbonized at 800 °C exhibits an intermediate capacity and severe kinetic restrictions. Consequently, the carbonization temperature threshold is set to 800 °C. Given the fact that there is a small transition range between low and high adsorption capacity, it is not reasonable to enhance the carbonization temperature steps to significantly more than 100 °C. As a result, the carbonization temperature thresholds can be assessed with an uncertainty of ±50 °C. However, a more detailed qualitative assessment of isotherms can improve the accuracy of a direct comparison of different gases. For example, N_2 and CO_2 (see isotherms in the Supporting Information) show a very similar adsorption behavior and were assigned the same carbonization temperature threshold of 900 °C; but for a carbonization temperature of 900 °C the isotherm of N_2 shows a more pronounced pseudo-hysteresis than CO_2, which indicates a significantly lower adsorption rate. Consequently, despite being assigned the same carbonization temperature threshold, CO_2 can be considered smaller than N_2.

Furthermore, in accordance with literature, it is expected that the molecular sieve effect is also temperature dependent. For example, nitrogen can enter pores at elevated temperature, from which it is excluded at cryogenic temperatures used for pore size analysis [21,72]. This effect is also visible in Ar adsorption for the samples studied here. At 87 K, the carbonization temperature threshold is 750 °C [67] but increases to 850 °C at 273 K (see Supporting Information). Furthermore, some measurements are not possible with a reasonable duration at the cryogenic temperatures used for pore size analysis (the measurement of a simple Ar sorption isotherm at 87 K takes more than 200 h [67] on this material). As a result, at cryogenic temperatures it is expected that kinetic restrictions become so severe that they will conceal size effects observed in equilibrium. Hence, the discussion in this work is restricted to 273 K, i.e., closer to room temperature and more relevant for technical separation applications.

4.2. Stability of the carbon molecular sieve

The long-term stability is an important property of any adsorbent for industrial processes. Two important aspects can be considered to describe the stability of a porous material.

First of all, the pore volume is important for the adsorption capacity and should stay constant over a high number of adsorption-desorption cycles. For this material, the adsorption capacity of CO_2 has been evaluated elsewhere [71]. It was found that the adsorption capacity is not reduced after 300 cycles [71].

Secondly, the pore size should be constant as it has a significant impact on the isotherm shape and, therefore, the design of an adsorption process. This is particularly important for a molecular sieve, where little changes in pore size can impact the adsorption capacity of small gas molecules in the size range of the pores. To verify that the carbon molecular sieves do not significantly change their pore size, H_2O and CO_2 adsorption measurements were reproduced on the same sample after 18 months and about 20 steps consisting of heat-assisted degassing (200 °C), adsorption and desorption. The original isotherms and their reproduction are shown in Fig. S3. It becomes apparent that the kinetic restrictions very close to the carbonization temperature threshold slightly improve, which is an indication for a widening of the pores. It must be emphasized, though, that the effect is too small to have an impact on the determination of carbonization temperature thresholds in subsequent measurements.

4.3. Relating carbonization temperature threshold and molecular dimensions

Fig. 3 shows the carbonization temperature threshold of adsorption for various adsorptives depending on their molecular dimension. The molecular dimensions are given as kinetic diameter (a), critical diameter (b) and MIN-1 (c). As the pore size is shrinking with increasing carbonization temperature, adsorptives with a small diameter are expected to show a high carbonization temperature threshold. Consequently, a concept which describes the experimental data correctly must give a continuous correlation between increasing molecular size and decreasing carbonization temperature threshold.

Fig. 3d shows the molecular size related to the adsorbate's ability to enter the ultramicropores. This order is purely qualitative and does not rely on the carbonization temperature threshold assignment.

For further analysis, Fig. 4 shows the differences in molecular size of all possible gas pairs of the adsorptives measured for this study as numerical value and in a color code. The adsorptives are ordered by their ability to enter pores with increasing carbonization temperature. Unlike the carbonization temperature threshold, this order is only qualitative. Adsorptives with a low difference in size exclusion behavior, i.e., close to the diagonal in the middle of the table are expected to show a low difference in molecular size. Molecular sieving in this regime is demanding and only kinetic separation appears possible rather than a real size exclusion effect. In the top right corner of the matrix, carbonization temperature threshold and the difference in molecular diameter are high. Consequently, synthesizing a molecular sieve for a gas pair is comparatively easy (green color). A molecular size concept ideally matching with the experimentally determined pore accessibility would result in a gradual change of the color from red (close to the diagonal in the middle) to green (top right corner). Deviations from ideal behavior are visible for example as fully red or fully green lines or columns or significant deviations in color in comparison to the surrounding fields.

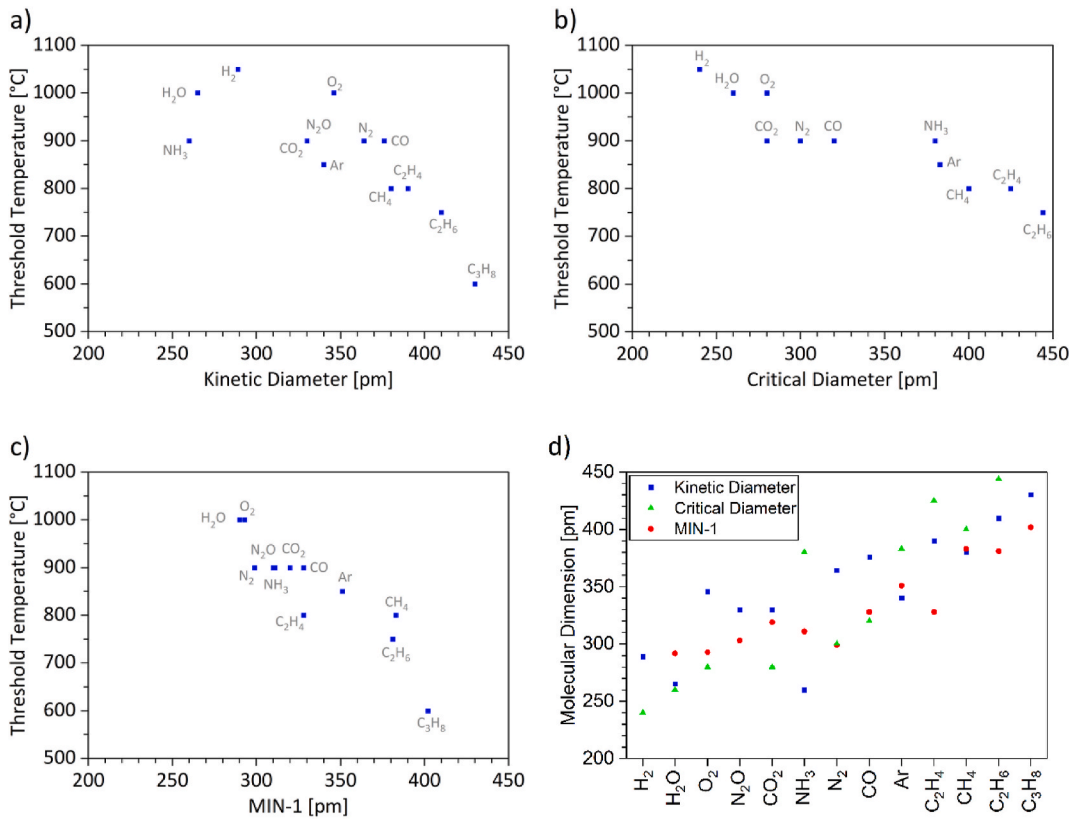

Fig. 3. Carbonization temperature threshold of the adsorption capacity depending on the molecular dimensions. Kinetic diameter by Breck [27] (a), and critical diameter listed by Grubner et al. [34] (b) and MIN-1 by Webster et al. [30,46–48] (c). In addition, all molecular dimensions are shown in (d) for different adsorptives. The adsorptives are ordered corresponding to their carbonization temperature threshold.

Fig. 4. Differences in molecular size for all possible combinations from the set of adsorptives measured for this study. The molecular sizes are given for the kinetic diameter (a), the critical diameter (b) and MIN-1 (c). The differences in molecular sizes are color-coded, which is shown as a legend in (d). The adsorptives are arranged by their carbonization temperature threshold. (For interpretation of the references to color in this figure legend, the reader is referred to the Web version of this article.)

Consequently, this representation allows to identify outliers easily.

In the following, firstly the consistency of the different concepts and experimental observations is discussed for some typical application scenarios of molecular sieves. Secondly, additional issues of these concepts emerging as outliers in Figs. 3 and 4 are discussed.

5. Discussion

5.1. Discussion of applications for molecular sieves

5.1.1. N_2/O_2

As mentioned previously, a common application for carbon molecular sieves is the separation of N_2 and O_2 in air. Typically, the kinetic diameter (O_2: 346 pm; N_2: 364 pm) [27] is cited to explain the adsorption behavior of these two gases [73]. On comparing these kinetic diameters to the critical diameter and MIN-1, it becomes apparent, that all three studied concepts for molecular dimensions consider O_2 to be a smaller molecule than N_2 (see Table 1 and Fig. 3d). This is confirmed by the adsorption behavior of the carbon nanofibers studied in this work and, obviously, by the existence of commercial carbon molecular sieves for air separation [5,8,74]. While both gases show a similar adsorption behavior, the carbonization temperature threshold is shifted from 900 °C (N_2) to 1000 °C (O_2) (see isotherms in the Supporting Information). This observation indicates that N_2 is kinetically hindered in pores that are still easily accessible by O_2. Consequently, N_2 is the larger molecule. All in all, experimental results and all studied concepts for the molecular size are consistent with each other for O_2 and N_2.

5.1.2. CH_4/CO_2

Another example for size exclusion in carbon molecular sieves is the separation of CH_4 and CO_2, for example for biogas purification [13]. To give evidence that these gases may be separated by a molecular sieve effect, the kinetic diameter (CH_4: 380 pm; CO_2: 330 pm) [27] is the concept of choice in the literature as well [11,75,76]. The critical diameter and MIN-1 predict larger dimensions for CH_4 in comparison to CO_2, too (Table 1, Fig. 3d). The adsorption behavior of both gases on the PAN-based carbon nanofibers confirms the comparatively large size difference of both molecules. Whereas CH_4 is excluded at carbonization temperatures above 800 °C, CO_2 can still adsorb in carbon fibers carbonized at 900 °C, but with a very slow adsorption rate [68] (see isotherms in the Supporting Information).

5.1.3. CH_4/N_2

The separation of N_2 from CH_4 is an important step for the purification of natural gas. As both N_2 and CH_4 are rather inert gases and show a difference in the kinetic diameter, molecular sieving appears to be a reasonable separation mechanism for adsorbent design. The difference in kinetic diameter is rather small (364 pm for N_2 vs. 380 pm for CH_4) [27]. In comparison, the difference in adsorption temperature thresholds on PAN-based carbon fibers is quite high (800 vs. 900 °C), which indicates that a separation with these fibers carbonized at 800 or 850 °C is expected to be possible with high selectivity. Various reports show that high selectivities can be obtained for CH_4/N_2 separations with dynamic gas adsorption [61,77] or in membranes [78,79]. Consequently, the higher difference in molecular size predicted by the critical diameter and MIN-1 may be a more realistic description.

5.1.4. CO_2/N_2

A molecular sieve separation of CO_2 and N_2 is discussed in literature [80], as the kinetic diameter of CO_2 is small (330 pm [27]) in comparison to N_2 (364 pm [27]). Consequently, the kinetic diameters of CO_2 and N_2 are often quoted to discuss if CO_2 will access pores when N_2 will not [67,76,80,81]. Having a look at the isotherms of CO_2 and N_2 for a carbonization temperature of 900 °C (see Supporting Information), it becomes apparent that N_2 can access the pores of the sample carbonized at 900 °C with similar kinetic restrictions like CO_2 at 273 K, although N_2 is considered larger by the concept of the kinetic diameter. The critical diameters of CO_2 (280 pm) and N_2 (300 pm) are much closer to each other, giving a better prediction of the observed size exclusion on the carbon molecular sieve. Hence, it must be emphasized that – also in ultramicroporous adsorbents – a much lower N_2 adsorption capacity in comparison to CO_2 is not necessarily a molecular sieve effect. Instead the difference in condensability (close to room temperature, CO_2 is below its critical temperature, N_2 is not; the evaporation temperature of CO_2 at 1 bar is much higher than for N_2) and chemical interactions must be taken into account, although it may be difficult to separate those effects on a single material. For the carbon molecular sieve studied here, the comparatively sudden change in adsorption capacity depending on the carbonization temperature allows to neglect any influence of surface chemistry, which changes gradually over the range of carbonization temperatures [67]. Overall, with the data presented here, it appears unlikely that an efficient molecular sieving of CO_2 and N_2 is possible without kinetic restrictions even for the smaller molecule. This is confirmed by the results of Liu et al. [61], who observed that the offset of kinetic restrictions for CO_2 and N_2 begins at the same pyrolysis severity.

5.1.5. Hydrocarbons

For other applications, the kinetic diameter also has some drawbacks. Especially for different isomers of hydrocarbons, shortcomings regarding the lack of different dimensions became apparent and are discussed elsewhere for adsorption on zeolites [21,22]. This application will not be discussed here, as hydrocarbons larger than propane will not adsorb in the ultramicropores of the studied carbon molecular sieve.

5.2. Discussion of concepts for molecular dimensions

5.2.1. Kinetic diameter

In addition to the separation applications discussed above, the kinetic diameter shows some additional deviations from the expected correlation of the molecular dimension and the carbonization temperature threshold, visible as outliers in the plot in Fig. 3a. For example, the kinetic diameter of CO is higher than indicated by its adsorption behavior on the carbon nanofibers. In direct comparison to the isoelectronic N_2, CO shows an almost indistinguishable adsorption behavior that indicates that there is no size difference between these two adsorptives. The difference in kinetic diameter between CO (376 pm) and N_2 (364 pm) could be caused by their different chemical properties of these two adsorptives. CO exhibits a dipole moment that is not present in N_2 and may not be reflected in the adsorption potential that was used to calculate the kinetic diameters. For the other isoelectronic pair of gases, N_2O and CO_2, the kinetic diameter is the same (330 pm), as is expected from the almost identical adsorption isotherms.

Also other adsorptives can have a very different size exclusion behavior, despite having similar kinetic diameters. For example, the O_2 molecule (346 pm) can easily access the very small pores of the sample carbonized at 900 °C, whereas the Ar atom with a very similar kinetic diameter (340 pm) is kinetically hindered already for the pores of the carbon fibers prepared 800 °C.

Furthermore, the NH_3 molecule has a remarkably low kinetic diameter that is even lower than H_2O and H_2. Regarding the size exclusion effect on carbon nanofibers, however, NH_3 behaves like the much "larger" CO_2 and N_2O, indicating that the value for the kinetic diameter of NH_3 is far too small. This deviation becomes also obvious in the color-coding of Fig. 4. Whereas most of the gases show the anticipated gradual change from green to red when approaching the diagonal, the kinetic diameter of NH_3 is much larger or much smaller in comparison to adsorptives with a comparable size exclusion behavior.

Like the kinetic diameter of H_2O, the value for NH_3 is derived by Hirschfelder, Curtiss and Bird (HCB) [25] from experimental data using the Stockmayer potential [28]. Both values are comparatively small in comparison to the values derived with other methods (see Figs. 3d and 4), indicating that it is an intrinsic property of the Stockmayer potential

[28] to yield very small kinetic diameters. This effect is confirmed by comparing the molecular dimensions of additional polar adsorptives like chloroform (HCB [25]: 298 pm; MIN-1 [30]: 461.3 pm) and chloromethane (HCB [25]: 343 pm; MIN-1 [5]: 396 pm). In most other cases, kinetic diameters are larger than MIN-1 (see Fig. 3d).

5.2.2. Critical diameter

In contrast to the kinetic diameter, the approach of a construction of molecules with van der Waals-radii allows to give molecular dimensions in three directions, rather than an average value. For the access in slit pores, only the smallest dimension of a molecule is relevant. Consequently, the critical diameters listed in various works [36,37,39] (Fig. 3b) works better in predicting the adsorption behavior of different adsorptives in comparison to the kinetic diameter. An obvious deviation is the large difference in critical diameters of CO_2 and NH_3, although their adsorption behavior is very similar. In contrast to the observed deviation of NH_3 in the kinetic diameter discussion, the critical diameter of the NH_3 molecule is larger. A more detailed discussion is hindered by the fact that it is not entirely clear how the critical diameter of NH_3 was obtained. In Figs. 3b and 4b it becomes apparent, that not only the critical diameter of NH_3 is too high, but the critical diameter of CO_2 is slightly too small.

5.2.3. MIN-1

In comparison to the kinetic diameter, the MIN-1 values computed by Webster et al. [30,46–48] do a better job as well in predicting the adsorption behavior of the adsorptives studied in this work. Small deviations from the linear relationship between carbonization temperature threshold and molecular dimension are solely found for the hydrocarbons C_2H_4 and C_3H_8. In contrast to the kinetic diameter, the MIN-1 by Webster et al. are derived from ab-initio calculations and not from macroscopic data that can only give an average value for three dimensions of a molecule. Hence, their accuracy is much better, as they take all three dimensions into account to estimate the overall smallest diameter of the molecule, which determines the accessibility of a slit pore. A notable exception is the small difference in MIN-1 of O_2 and N_2, which is not reflected in the size exclusion behavior observed in the isotherms. On comparing Fig. 4b and c it attracts attention that the differences in molecular dimensions are much smaller for MIN-1 than for critical diameters, resulting in a color shift towards red and orange.

5.3. Perspectives with PAN-based carbon nanofibers

Using the relation of molecular size and carbonization temperature threshold, it appears possible to tailor the carbonization temperature of electrospun PAN-based carbon nanofibers to optimal performance for O_2/N_2, CO_2/CH_4 or N_2/CH_4 separation. Other separation problems like C_2H_4/C_2H_6 may be tackled as well, given that a difference in molecular size is present. This necessary difference is expected to be as low as 20 pm (in critical diameter), since the size difference of the O_2 and N_2 molecules is that small and a commercial molecular sieve for this application is available. To evaluate the performance of tailored electrospun PAN-based carbon nanofibers in these and other separation problems will be part of future investigations.

6. Conclusion

Molecular dimensions of gases are needed for various applications, be it for the separation of gases in molecular sieves or characterization of materials using molecular probes. In this work, commonly used methods to estimate the size of gas molecules were evaluated using a tailorable carbon molecular sieve. For specific applications for molecular sieves like CO_2/CH_4 and O_2/N_2 the different methods showed consistent results with the experimental observations on the tailorable carbon molecular sieve. However, it was shown that the widely applied kinetic diameter shows some drawbacks, especially for polar molecules. More consistent results were obtained with the critical diameter and the concept of MIN-1 and MIN-2 introduced by Webster. Finally, as a result, the possibility to steplessly tailor PAN-based carbon nanofibers may allow to synthesize a carbon molecular sieve for any gas separation application with sufficient difference in molecular sizes.

CRediT authorship contribution statement

A. Kretzschmar: Writing – original draft, Visualization, Methodology, Investigation, Conceptualization. **V. Selmert:** Writing – review & editing, Validation, Conceptualization. **H. Kungl:** Writing – review & editing, Visualization, Supervision, Project administration, Funding acquisition, Conceptualization. **H. Tempel:** Writing – review & editing, Supervision, Project administration, Funding acquisition, Conceptualization. **R.-A. Eichel:** Writing – review & editing, Supervision, Project administration, Funding acquisition, Conceptualization.

Declaration of competing interest

The authors declare the following financial interests/personal relationships which may be considered as potential competing interests: Hermann Tempel, Ansgar Kretzschmar, Victor Selmert, Hans Kungl and Rüdiger-A. Eichel have patent #WO2020249441A1 issued to Forschungszentrum Jülich.

Data availability

Data will be made available on request.

Acknowledgement

The authors acknowledge funding provided by the Deutsche Forschungsgemeinschaft (DFG, German Research Foundation) under Germany's Excellence Strategy – Cluster of Excellence 2186 "The Fuel Science Center" – ID: 390919832.

Appendix A. Supplementary data

Supplementary data to this article can be found online at https://doi.org/10.1016/j.micromeso.2022.112156.

List of acronyms

FCC	Fluid Catalytic Cracking
MOF	Metal Organic Framework
TEM	Transmission Electron Microscopy
ZINDO	Zerner's Intermediate Neglect of Differential Overlap

References

[1] D.B.G. Williams, M. Lawton, J. Org. Chem. 75 (2010) 8351–8354.
[2] D.R. Burfield, R.H. Smithers, J. Org. Chem. 48 (1983) 2420–2422.
[3] D.R. Burfield, R.H. Smithers, J. Org. Chem. 43 (1978) 3966–3968.
[4] P. Mazzei, F. Minichiello, D. Palma, Appl. Therm. Eng. 25 (2005) 677–707.
[5] C.R. Reid, K.M. Thomas, J. Phys. Chem. B 105 (2001) 10619–10629.
[6] T.D. Burchell, O.O. Omatete, N.C. Gallego, F.S. Baker, Adsorpt. Sci. Technol. 23 (2005) 175–194.
[7] R.T. Yang, Adsorbents: Fundamentals and Applications, John Wiley & Sons, Inc, Hoboken, NJ, USA, 2003.
[8] H. Heimbach, H. Jüntgen, K. Knoblauch, W. Körbächer, H. Münzer, W. Peters, D. Zündorf, Kohlenstoffhaltige molekularsiebe. https://patents.google.com/patent/DE2119829B2/de.
[9] N. Böcker, M. Grahl, A. Tota, P. Häussinger, P. Leitgeb, B. Schmücker, In: Ullmann's Encyclopedia of Industrial Chemistry, Wiley-VCH Verlag GmbH & Co. KGaA, Weinheim, Germany, 2000, pp. 1–27.
[10] T. Montanari, E. Finocchio, E. Salvatore, G. Garuti, A. Giordano, C. Pistarino, G. Busca, Energy 36 (2011) 314–319.
[11] Z. Bacsik, O. Cheung, P. Vasiliev, N. Hedin, Appl. Energy 162 (2016) 613–621.
[12] F. Ferella, A. Puca, G. Taglieri, L. Rossi, K. Gallucci, J. Clean. Prod. 164 (2017) 1205–1218.

[13] R.L.S. Canevesi, K.A. Andreassen, E.A. da Silva, C.E. Borba, C.A. Grande, Ind. Eng. Chem. Res. 57 (2018) 8057–8067.
[14] A. Behr, D.W. Agar, J. Jörissen, A.J. Vorholt, Einführung in die Technische Chemie, 2. Auflage, Springer Spektrum, Berlin, 2016.
[15] R.T. Yang, Gas Separation by Adsorption Processes, Elsevier Science, Burlington, 1987.
[16] J.P. Jampol'skij, B.D. Freeman, I. Pinnau (Eds.), Materials Science of Membranes for Gas and Vapor Separation, Reprinted with Corr, Wiley, Chichester, 2007.
[17] R.W. Baker, Membrane Technology and Applications, third ed., Wiley-Blackwell, Oxford, 2012.
[18] A.F. Ismail, K.C. Khulbe, T. Matsuura, Gas Separation Membranes: Polymeric and Inorganic, Springer, Cham, 2015.
[19] Z. Hu, N. Maes, E.F. Vansant, J. Porous Mater. 2 (1995) 19–23.
[20] K.S. Sing, R.T. Williams, Part. Part. Syst. Char. 21 (2004) 71–79.
[21] Y. Traa, J. Weitkamp, in: F. Schüth, K.S. Sing, J. Weitkamp (Eds.), Handbook of Porous Solids, Wiley-VCH Verlag GmbH, Weinheim, Germany, 2002, pp. 1015–1057.
[22] Y. Traa, S. Sealy, in: H.G. Karge, J. Weitkamp (Eds.), J. Weitkamp, Characterization II, Springer Berlin Heidelberg, 2006, pp. 103–154.
[23] M. Helmich, M. Luckas, C. Pasel, D. Bathen, Chem. Ing. Tech. 84 (2012) 1391–1392.
[24] S.H. Madani, A. Silvestre-Albero, M.J. Biggs, F. Rodríguez-Reinoso, P. Pendleton, Chemphyschem a European journal of chemical physics and physical chemistry 16 (2015) 3984–3991.
[25] J.O. Hirschfelder, C.F. Curtiss, R.B. Bird, Molecular Theory of Gases and Liquids, Corr. Print. With Notes Added, Wiley, New York,NY, 1964.
[26] R.A. Svehla, NASA Tech. Rep. R-132, 1962. https://ntrs.nasa.gov/citations/19630012982.
[27] D.W. Breck, Zeolite Molecular Sieves: Structure, Chemistry, and Use, Wiley, New York, 1974.
[28] W.H. Stockmayer, J. Chem. Phys. 9 (1941) 398–402.
[29] L. Pauling, The Nature of the Chemical Bond and the Structure of Molecules and Crystals: an Introduction to Modern Structural Chemistry, vol. 2, Cornell Univ. Press, Ithaca, New York, 1940.
[30] C.E. Webster, R.S. Drago, M.C. Zerner, J. Am. Chem. Soc. 120 (1998) 5509–5516.
[31] S.K. Lilov, Cryst. Res. Technol. 21 (1986) 1299–1302.
[32] I.A. Sokolova, V.E. Liousternik, in: In: AIP Conference Proceedings, AIP, 13-18 Aug 1995, pp. 167–170.
[33] B.E. Poling, J.M. Prausnitz, J.P. O'Connell, Properties of Gases and Liquids, Fifth edition, fifth ed., McGraw-Hill Education, New York, N.Y., 2020. McGraw Hill.
[34] O. Grubner, P. Jiru, M. Ralek, Molekularsiebe, VEB Deutscher Verlag der Wissenschaften, Berlin, 1968.
[35] M. Ralek, P. Jiru, O. Grubner, Molekulová Síta, Státni nakladatelství technické literatury, Praha, 1966.
[36] W. Kast, Adsorption aus der Gasphase: Ingenieurwissenschaftliche Grundlagen und technische Verfahren, VCH, Weinheim, 1988.
[37] H.-J. Bart, U. von Gemmingen, In: Ullmann's Encyclopedia of Industrial Chemistry, Wiley-VCH Verlag GmbH & Co. KGaA, Weinheim, Germany, 2000.
[38] A. Schönbucher, Thermische Verfahrenstechnik: Grundlagen und Berechnungsmethoden Für Ausrüstungen und Prozesse, Springer Berlin/Heidelberg, Berlin, Heidelberg, 2002.
[39] E. Smolková-Keulemansová (Ed.), Analysis of Substances in the Gaseous Phase, Elsevier, Amsterdam, New York, 1991.
[40] Merck, Molecular Sieves: Mineral Adsorbents, Filter Agents, and Drying Agents, 25 November 2021. https://www.sigmaaldrich.com/DE/de/technical-documents/technical-article/chemistry-and-synthesis/reaction-design-and-optimization/molecular-sieves.
[41] Vurup, Molecular Sieves SLOVSIT, 25 November 2021. https://www.vurup.sk/en/services/production/molecular-sieves-slovsit/.
[42] R.M. Barrer, Trans. Faraday Soc. 40 (1944) 555.
[43] R.M. Barrer, Trans. Faraday Soc. 45 (1949) 358.
[44] J.C. Slater, Introduction to Chemical Physics, McGraw-Hill, New York, 1939.
[45] H. Schoen, Handbuch der Reinsten Gase, Springer Berlin/Heidelberg, Berlin, Heidelberg, 2005.
[46] C.E. Webster, R.S. Drago, M.C. Zerner, J. Phys. Chem. B 103 (1999) 1242–1249.
[47] C.E. Webster, A. Cottone, R.S. Drago, J. Am. Chem. Soc. 121 (1999) 12127–12139.
[48] C.E. Webster, Modeling Adsorption: Investigating Adsorbate and Adsorbent Properties, PhD thesis, 1999.
[49] M.C. Zerner, ZINDO, Department of Chemistry, University of Florida, Gainesville, FL 32611.
[50] J.L. Pascual-Ahuir, E. Silla, J. Comput. Chem. 11 (1990) 1047–1060.
[51] E. Silla, I. Tuñón, J.L. Pascual-Ahuir, J. Comput. Chem. 12 (1991) 1077–1088.
[52] J.L. Pascual-ahuir, E. Silla, I. Tuñon, J. Comput. Chem. 15 (1994) 1127–1138.
[53] D.M. Ruthven, Separ. Purif. Methods 5 (1976) 189–246.
[54] N. Mehio, S. Dai, D. Jiang, J. Phys. Chem. A 118 (2014) 1150–1154.
[55] H.A. Stuart, Die Struktur des Freien Moleküls: Allgemeine Physikalische Methoden zur Bestimmung der Struktur von Molekülen und ihre Wichtigsten Ergebnisse, Springer, Berlin, Heidelberg, 1952.
[56] V. Teplyakov, P. Meares, Gas Separ. Purif. 4 (1990) 66–74.
[57] L.M. Robeson, B.D. Freeman, D.R. Paul, B.W. Rowe, J. Membr. Sci. 341 (2009) 178–185.
[58] M.M. Dal-Cin, A. Kumar, L. Layton, J. Membr. Sci. 323 (2008) 299–308.
[59] T. Kihara, J. Phys. Soc. Jpn. 6 (1951) 289–296.
[60] J. Liu, Y. Liu, D. Kayrak Talay, E. Calverley, M. Brayden, M. Martinez, Carbon 85 (2015) 201–211.
[61] J. Liu, C. Han, M. McAdon, J. Goss, K. Andrews, Microporous Mesoporous Mater. 206 (2015) 207–216.
[62] J.N. Barsema, N.F.A. van der Vegt, G.H. Koops, M. Wessling, J. Membr. Sci. 205 (2002) 239–246.
[63] T. Tomita, K. Nakayama, H. Sakai, Microporous Mesoporous Mater. 68 (2004) 71–75.
[64] S.H. Madani, M.J. Biggs, F. Rodríguez-Reinoso, P. Pendleton, Microporous Mesoporous Mater. 278 (2019) 232–240.
[65] S.H. Madani, P. Kwong, F. Rodríguez-Reinoso, M.J. Biggs, P. Pendleton, Microporous Mesoporous Mater. 264 (2018) 76–83.
[66] Y.P. Yampolskii, B.D. Freeman, Membrane Gas Separation, Wiley, Hoboken, NJ, 2010.
[67] A. Kretzschmar, V. Selmert, H. Weinrich, H. Kungl, H. Tempel, R.-A. Eichel, ChemSusChem 13 (2020) 3180–3191.
[68] A. Kretzschmar, V. Selmert, H. Weinrich, H. Kungl, H. Tempel, R.-A. Eichel, Chem. Eng. Technol. 44 (2021) 1168–1177.
[69] R. Schierholz, D. Kröger, H. Weinrich, M. Gehring, H. Tempel, H. Kungl, J. Mayer, R.-A. Eichel, RSC Adv. 9 (2019) 6267–6277.
[70] J. Park, A. Kretzschmar, V. Selmert, O. Camara, H. Kungl, H. Tempel, S. Basak, R. A. Eichel, ACS Appl. Mater. Interfaces 13 (39) (2021) 46665–46670, https://doi.org/10.1021/acsami.1c13541.
[71] V. Selmert, A. Kretzschmar, H. Weinrich, H. Tempel, H. Kungl, R.-A. Eichel, ChemSusChem (2022), e202200761.
[72] S.J. Gregg, M.I. Pope, Fuel 38 (1959) 501.
[73] S.P. Nandi, P.L. Walker, Separ. Sci. 11 (1976) 441–453.
[74] M.M. Hassan, D.M. Ruthven, N.S. Raghavan, Chem. Eng. Sci. 41 (1986) 1333–1343.
[75] X.Y. Chen, H. Vinh-Thang, A.A. Ramirez, D. Rodrigue, S. Kaliaguine, RSC Adv. 5 (2015) 24399–24448.
[76] Y. Zhao, X. Liu, Y. Han, RSC Adv. 5 (2015) 30310–30330.
[77] O. Gorska, A.W. Cyganiuk, A. Olejniczak, A. Ilnicka, J.P. Lukaszewicz, Open Chemistry 13 (2015).
[78] K. Hazazi, X. Ma, Y. Wang, W. Ogieglo, A. Alhazmi, Y. Han, I. Pinnau, J. Membr. Sci. 585 (2019) 1–9.
[79] X. Ning, W.J. Koros, Carbon 66 (2014) 511–522.
[80] M. Oschatz, M. Antonietti, Energy Environ. Sci. 11 (2018) 57–70.
[81] M.R. Hudson, W.L. Queen, J.A. Mason, D.W. Fickel, R.F. Lobo, C.M. Brown, J. Am. Chem. Soc. 134 (2012) 1970–1973.